
HVL: Semi-Supervised Segmentation leveraging Hierarchical Vision-Language Synergy with Dynamic Text-Spatial Query Alignment

Numair Nadeem*
University of Regina
Regina, Canada
nng794@uregina.ca

Saeed Anwar
The University of Western Australia
Perth, Australia
saeed.anwar@uwa.edu.au

Muhammad Hamza Asad
University Canada West
Vancouver, Canada
muhammadhamza.asad@ucanwest.ca

Abdul Bais
University of Regina
Regina, Canada
abdul.bais@uregina.ca

Abstract

In this paper, we address Semi-supervised Semantic Segmentation (SSS) under domain shift by leveraging domain-invariant semantic knowledge from text embeddings of Vision-Language Models (VLMs). We propose a unified Hierarchical Vision-Language framework (**HVL**) that integrates domain-invariant text embeddings as object queries in a transformer-based segmentation network to improve generalization and reduce misclassification under limited supervision. The mentioned textual queries are used for grouping pixels with shared semantics under SSS. HVL is designed to (1) generate textual queries that maximally encode domain-invariant semantics from VLM while capturing intra-class variations; (2) align these queries with spatial visual features to enhance their segmentation ability and improve the semantic clarity of visual features. We also introduce targeted regularization losses that maintain vision-language alignment throughout training to reinforce semantic understanding. HVL establishes a novel state-of-the-art by achieving a +9.3% improvement in mean Intersection over Union (mIoU) on COCO, utilizing 232 labelled images, +3.1% on Pascal VOC employing 92 labels, +4.8% on ADE20 using 316 labels, and +3.4% on Cityscapes with 100 labels, demonstrating superior performance less than 1% supervision on four benchmark datasets. Our results show that language-guided segmentation bridges the label efficiency gap and enables new levels of fine-grained generalization.

1 Introduction

Developing semantic segmentation models with minimal dependence on labelled data continues to be a significant challenge in computer vision. This is particularly true in autonomous driving, agriculture, and medical imaging, where acquiring dense pixel-level annotations is expensive and time-intensive. Semi-supervised Semantic Segmentation (SSS) addresses this issue by leveraging a small set of labelled images alongside a large pool of unlabelled data, aiming to achieve strong performance without full supervision. Typical strategies include adversarial training Mittal et al. [2019], and self-training Souly et al. [2017], Yang et al. [2023b, 2022], which aim to extract supervisory signals from unlabelled data.

*Corresponding author

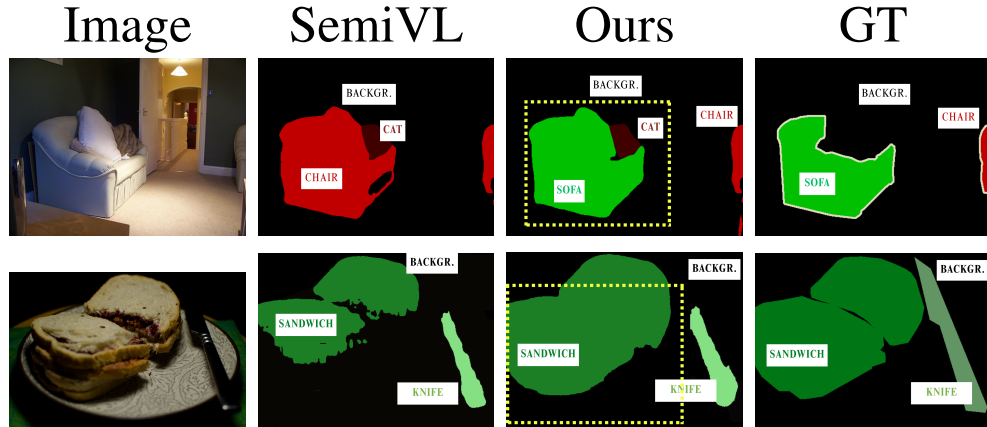


Figure 1: Example predictions: First row is on Pascal VOC with 92 labels, and the second row is for COCO with 232 labels. Our method accurately disambiguates similar classes, reduces over-segmentation, and produces sharp boundaries.

While recent SSS methods Hoyer et al. [2024], Yang et al. [2025b] produced accurate boundaries, they often suffer from misclassification, particularly in cases involving visually similar classes or significant class-appearance variation. For example, confusing sofas with chairs (see Fig. 1) due to poor representation of rare classes in the labelled subset Zhong et al. [2023]. These shortcomings highlight the need for improved semantic understanding and grounding in low-annotation regimes Yang et al. [2023b].

The current advancements in VLMs Fang et al. [2023], Liu et al. [2023] have opened new avenues for improving semantic understanding with limited supervision. Trained through large-scale image-text contrastive learning, VLMs encode rich, domain-invariant semantic representations that are effective in image classification tasks Abdelfattah et al. [2023] through the alignment of visual content with textual descriptions within a shared embedding space. For example, when given an image of a red car and several candidate captions, the model learns to bring the correct pairing (“a red car”) closer together in the shared space while pushing mismatched pairs apart. This training objective enables robust vision-language alignment and generalization across diverse domains. Motivated by this success, recent studies have explored using VLM-derived text embeddings to guide pixel-level predictions in semantic segmentation. These embeddings provide a way to incorporate high-level semantic cues into the training process. However, since they are learned at the image level for classification tasks, these embeddings lack spatial detail, often resulting in coarse and noisy masks when applied directly to segmentation tasks Hoyer et al. [2024].

Despite progress in SSS and VLMs, the current SSS methods are based solely on vision-based features, limiting their semantic expressiveness for rare or ambiguous classes French et al. [2019]. VLMs offer complementary strengths, providing class-level priors, but lacking spatial understanding Chen et al. [2023a]. Current frameworks rarely fuse these strengths, leading to persistent challenges such as misclassification and weak boundary delineation. Although some works have started incorporating textual representations from VLM into SSS frameworks Hoyer et al. [2024], focusing mainly on visual features and do not fully exploiting language-based supervision, where textual embeddings guide segmentation, we propose HVL, a language query-based framework combining vision models’ spatial precision with VLMs’ semantic richness to enhance generalization, class discrimination, and label efficiency in low-annotation regimes.

HVL’s goal is to utilize and enhance domain-invariant class-level text embeddings from VLMs as object queries, termed as textual queries, which would serve as semantic anchors to group pixels belonging to the same class across diverse domains. To achieve this, it is designed to generate semantically rich and image-relevant textual queries and enhance their alignment with visual features for improved localization and class separation. Our contributions can be summarized as follows:

- To the best of our knowledge, we are the first to introduce a language-driven SSS framework that explicitly leverages textual embeddings as object queries from VLMs with image-specific enhancements to guide mask predictions under limited supervision.

- We propose a unified vision-language architecture that enables language-derived queries to interact more effectively with pixel-level features. This is achieved through a structured decoding process that progressively bridges the semantic gap between global language cues and localized visual details, enabling improved class discrimination, generalization across domains, and robustness in low-annotation regimes.

2 Related Works

Semi-supervised Semantic Segmentation (SSS) addresses the challenge of training segmentation models with limited pixel-level annotations Chi et al. [2024], Nadeem et al. [2025a,b], Yuan et al. [2024], Zhao et al. [2024]. Early approaches explored adversarial training frameworks, where the segmentation model acted as a generator aiming to produce label-like outputs that could fool a discriminator Chen et al. [2021], Wu et al. [2023]. Although these methods were innovative, they were challenging to train and lacked stability Yang et al. [2025b].

Subsequent work has shifted to simpler frameworks that focus on entropy minimization Zou et al. [2021] and consistency regularization Guan et al. [2022], Yang et al. [2023a], forming the backbone of most recent methods. These techniques rely on self-training, where the model iteratively generates and refines pseudo-labels for unlabelled data, enforcing prediction stability under various augmentations. One influential direction, introduced by French et al. [2020], employs Cutout and CutMix Yun et al. [2019] on unlabelled images to enhance generalization. Later, Cross Pseudo Supervision (CPS) Chen et al. [2021] revealed that CutMix works more efficiently with a co-training strategy, where two segmentation networks exchange pseudo-labels to supervise each other mutually. Adaptive Equalization Learning (AEL) Hu et al. [2021] refined this by proposing adaptive CutMix, biasing data towards under-performing classes. However, these methods faced challenges in early-stage pseudo-label quality. Therefore, ST++ Liu et al. [2022] and SimpleBaseline Yuan et al. [2021] adopted staged pseudo-label augmentation, gaining promising results but sacrificing simplicity.

Recent approaches, notably UniMatch-v2 Yang et al. [2025a], and iMAS Zhao et al. [2023], leveraged confidence thresholds for pseudo-labels inspired by FixMatch Sohn et al. [2020]. UniMatch-v2 emphasized dual-stream augmentations, where the same unlabelled image is passed through both weak and strong augmentations in parallel streams to enforce prediction consistency and improve generalization. These simpler methods influenced future developments, including SemiVL Hoyer et al. [2024]. SemiVL used a regularization framework and CLIP Radford et al. [2021b] text embeddings to guide visual features. However, it relied on abstract embeddings without refining them based on input images or using them as object queries to group pixels by class. This constrained the model’s effectiveness and segmentation performance.

Vision-Language Models. VLMs use large-scale image–text pretraining to create a shared embedding space between visual content and language. This enables VLMs to generalize across vision tasks, including image classification, retrieval, and open-vocabulary recognition. Their performance improves further with prompt engineering, text augmentation Zhou et al. [2022b,c], prompt ensembling, or LLM-generated class descriptions. Recent works extend VLMs to semantic segmentation through two main directions. Zero-shot segmentation methods Xu et al. [2022], Zhou et al. [2022a] rely solely on image–text pairs to generate segmentation masks without dense supervision. However, these masks are typically coarse and noisy due to the lack of pixel-level annotations. To improve mask quality, open-vocabulary segmentation approaches like ZegCLIP Zhang et al. [2023b] align dense visual features with text embeddings using learned decoders or attention mechanisms. Parameter-efficient tuning techniques—such as prompt tuning Jia et al. [2022], and partial fine-tuning Tao et al. [2023]—further help improve generalization while preventing overfitting.

Recently, EVA-CLIP Fang et al. [2023] incorporated masked image modeling for denser supervision, while LLaVA Liu et al. [2023] and InternVL Chen et al. [2023b] enabled open-ended reasoning and visual dialogue that also benefit segmentation tasks. In contrast to these lines of work, our method uniquely focuses on SSS, aiming to enhance generalization under limited pixel-level supervision.

Query Design Strategies. Transformer-based segmentation models adopted query-driven architectures, where object queries—learned embeddings—are passed through a transformer decoder with pixel features to detect and segment objects Vaswani et al. [2017]. Each query focuses on a specific object or class, acting as a latent anchor that aggregates relevant spatial features. Hence, the model *implicitly* localizes and extracts regions via attention mechanisms. To enhance effectiveness, prior

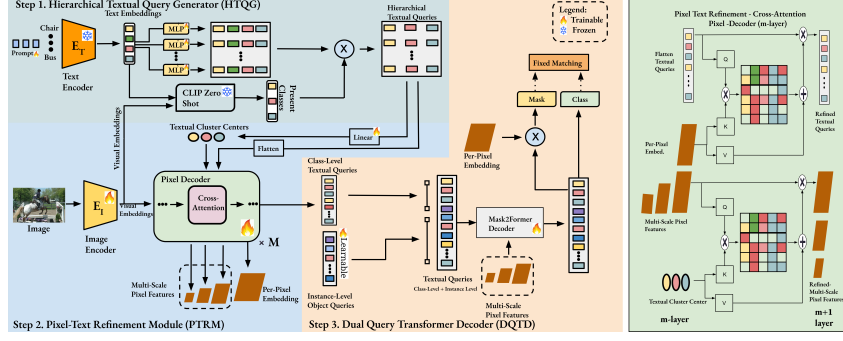


Figure 2: The CLIP image encoder extracts visual embeddings, while the frozen text encoder—prompted with class names—produces textual embeddings. (Step 1) The Hierarchical Textual Query Generator (HTQG) creates class-specific textual queries using separate MLP heads. Irrelevant class queries are filtered using CLIP zero-shot predictions. (Step 2) The selected hierarchical queries are projected into cluster centers and aligned with multi-scale pixel features via cross-attention in the pixel decoder. This alignment enhances the semantic clarity of pixel features, thus improving segmentation by enabling queries to group spatial regions belonging to the same class. (Step 3) To model intra-class variations, the class-level queries are fused with randomly initialized instance-level object queries. These combined queries are refined through the Mask2Former decoder, along with final pixel embeddings, to generate per-query masks and class labels. Each prediction output is then assigned to its corresponding ground truth (GT) through fixed matching, ensuring that each query consistently represents the semantic information of one class.

works introduced various strategies. For example, kMaX-DeepLab Yu et al. [2022] generates object queries from coarse segmentation masks, with each query carrying spatial priors about its region. This helps associate queries with relevant semantic areas. Several other approaches Zhang et al. [2023a] apply auxiliary supervision on object queries for better training stability, while some Kamath et al. [2021] explore conditional queries for adaptation across input modalities.

Building on these ideas, Mask2Former Cheng et al. [2022] uses masked cross-attention to restrict each query’s attention to a subset of the features corresponding to the predicted mask region, thereby improving spatial precision and reducing distractions from irrelevant areas. These object queries are randomly initialized and combined with multi-scale pixel features from a pixel decoder. They are then refined through a transformer decoder to generate segmentation masks. Existing query-based segmentation methods like Mask2Former face limitations because object queries are randomly initialized and learned without a semantic prior, which makes it difficult to consistently group pixels of the same class, especially when pixel features lack semantic consistency. Without a domain-invariant semantic space, features do not align well with queries, reducing segmentation quality. These issues worsen in SSS with limited data. Our work addresses SSS by designing domain-invariant object queries and a decoder framework to enhance their adaptability.

Textual Queries. Since VLMs learn to align free-form text with a vast array of web images, the class text embeddings obtained from them encode class semantics that have the potential to align visual features and could be utilized for semantic-segmentation under low annotation regimes as these embeddings remain reliable under changes in viewpoint, style, and domain Radford et al. [2021a]. When these embeddings are used as object queries in a segmentation transformer, each query contributes two built-in strengths: it supplies class-specific semantic prior knowledge that helps the model recognize the object, and it reflects many visual domains, giving the model a boost of domain robustness Pak et al. [2024]. Therefore, we utilize text embeddings from VLM as object queries containing domain-invariant priors instead of randomly initialized object queries with no semantic prior as in Cheng et al. [2022]. We improve pixel features clarity by refining them with textual queries in a pixel decoder, enabling better grouping by queries in the transformer decoder.

3 Methodology

We present HVL, a vision-language segmentation framework that utilizes domain-invariant semantic knowledge from CLIP in the form of textual queries to group pixels belonging to the same class. Additionally, we introduce regularization losses to align textual and visual queries. Our proposed

framework aims to leverage textual object queries for SSS. It adopts CLIP as a multi-modal backbone to extract textual and visual features. The image encoder E_I (ViT-B/16) is fine-tuned for dense predictions, producing multi-scale pixel features and global visual embedding $F_{\text{pixel}} \in \mathbb{R}^{H \times W \times D}$ projected into a shared vision-language space. For fine-tuning, we apply standard cross-entropy loss for labelled images, while for unlabelled images, we apply consistency regularization similar to SemiVL, encouraging predictions to remain stable under data augmentations. To effectively utilize textual queries for SSS, we build upon Mask2Former as our baseline with key changes. Firstly, the Hierarchical Textual Query Generator generates multi-scale textual queries that maximally encode domain-invariant semantic knowledge. Pixel-Text Refinement Module improves the segmentation capability of these queries by grounding them in the spatial structure of the image and injecting class-level semantics from queries into the visual features, and fusing instance-level queries with refined textual queries to capture intra-class variations. Lastly, following the practices of mask transformer, a transformer decoder refines the object and instance queries for the final mask prediction as demonstrated in Fig. 2.

Hierarchical Textual Query Generator (HTQG). To generate effective textual queries, we focus on preserving domain-invariant semantic knowledge of the queries and adapting them to the task and image context. Using CLIP as the backbone, we freeze the text encoder E_T to retain its pretrained semantic space, ensuring robust generalization across domains. To inject task-specific adaptability, we apply learnable prompts to refine the textual embeddings. For each class k , we apply a learnable prompt p and obtain the class-level text embedding as $t_k = E_T([p, \text{class}_k]) \in \mathbb{R}^C$. However, in dense segmentation tasks—especially under open-set or semi-supervised conditions—uniformly applying all class-level textual queries to every image is suboptimal. Moreover, queries for classes absent in an image introduce semantic noise, dilute attention, and degrade segmentation quality. Moreover, single-level textual embeddings struggle with intra-class variations, limiting their effectiveness in diverse visual contexts.

To address these limitations, HTQG filters class queries based on their presence in the current image and projects each valid class embedding into multiple levels of abstraction, from fine to coarse, to capture semantic variability better. Specifically, each embedding t_k is transformed by L distinct MLP heads, each tied exclusively to pixel features $z_l, l = 1, \dots, L$, at a corresponding resolution level inside the pixel-decoder to produce queries. $q_k^{(l)} = \text{MLP}_l(t_k) \in \mathbb{R}^D, l = 1, \dots, L$. This projection enables the model to reason across different semantic levels. For example, for the class “dog,” coarse-level queries may represent the general body structure, while fine-level queries capture localized details such as fur texture or ear shape. Moreover, to explicitly reinforce semantic differentiation

across query levels, we introduce a diversity regularization term: $\mathcal{L}_{\text{div}} = \sum_{l \neq l'} \left\| \frac{(q_k^{(l)})^\top q_k^{(l')}}{\|q_k^{(l)}\| \cdot \|q_k^{(l')}\|} \right\|_2^2$, penalizing similarity between queries from different semantic levels. This loss ensures each MLP head learns unique, complementary semantics rather than redundant features. To focus attention on classes actually present in an image, we use CLIP in a zero-shot manner to compute the semantic relevance of each class. For labelled images, we directly use the ground truth to select active classes. For unlabelled images, we extract an image embedding via CLIP and compute its similarity with class embeddings to estimate class presence probabilities. These relevance scores s_k modulate the initial textual queries, producing the final set of refined hierarchical queries: $Q^{\text{text}} = \{\tilde{q}_k^{(l)} = s_k \cdot q_k^{(l)}\} \in \mathbb{R}^{K \times L \times D}$.

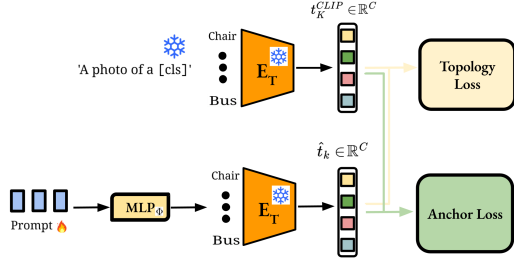


Figure 3: Query Regularization to Preserve Domain-Invariant Semantics of Text Embeddings

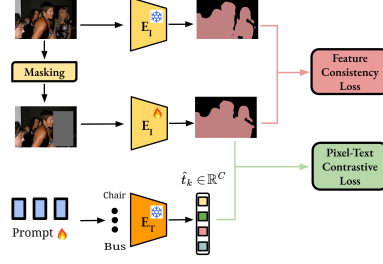


Figure 4: Semantic Supervision: stabilizes masked and reference features while reinforcing pixel-text alignment.

Pixel-Text Refinement Module (PTRM). While hierarchical textual queries encode domain-invariant class semantics, effective segmentation requires grounding them in the spatial structure of the input image. In contrast, pixel features $z_l \in \mathbb{R}^{H_l \times W_l \times D}$ contain rich local detail but lack explicit semantic clarity. To bridge this modality gap and improve the segmentation capabilities of textual queries, PTRM introduces a bidirectional cross-attention mechanism within the pixel decoder enabling mutual refinement.

To enrich the semantic representation of pixel features, PTRM applies a text-to-pixel attention strategy (see in Fig. 2). This alignment allows pixel features to be represented in terms of domain-invariant semantics, making them more effectively clusterable by the corresponding textual queries. To achieve this, we begin by generating textual cluster centers $c_t^{(l)} \in \mathbb{R}^{K \times D}$ for each query resolution level l , derived by linearly projecting the textual queries Q_t^{text} . These cluster centers serve as class-level semantic anchors corresponding to the pixel features z_l . Within the pixel decoder, for text-to-pixel attention, we utilize multi-scale pixel features $z^{(l)} \in \mathbb{R}^{L \times D}$ as query tokens Q_z with a linear projection. The textual queries Q_t^{ext} are similarly projected to key vectors K_t and value vectors V_t . We then compute the attention weights between pixel queries and textual keys: $W = \text{softmax}(Q_z K_t^T)$, and use them to refine the pixel features: $z_l \leftarrow z_l + W V_t$. We interpret the text-to-pixel attention mechanism as a way to guide pixel features toward alignment with the K textual clustering centers. The attention weights capture the semantic similarity between each of the L pixel features and the K textual query at each level l . The pixel features are refined using these weights through a weighted combination of the value vectors V_t . This refinement encourages pixels associated with the same class to cluster together, thereby enhancing the semantic consistency of the feature representations.

Conversely, the refined pixel features guide the textual queries: each query attends to the features to gather visual cues from relevant locations. This enriches the queries with boundary and layout information, sharpening mask predictions and improving localization. The final output of PTRM includes both: (i) enhanced pixel features z_l enriched with class semantics, and (ii) refined queries $Q_{\text{aligned}} = \{\hat{q}_k^{(l)}\}$, where $k = 1, \dots, K$; $l = 1, \dots, L$ informed by image-specific spatial context. These are passed to the dual-query transformer decoder for final segmentation.

Dual-Query Transformer Decoder (DQTD). While class-level K textual queries provide strong semantic supervision. However, variations in appearance or visual similarity between instances of the same class and their surroundings can lead to misclassification. To address this, we incorporate multiple learnable instance-level queries, randomly initialized as object queries, that interact with image features to capture multiple instances of a class and their diverse appearances. These queries provide different perspectives of the same class, allowing the model to recognize these instances as one class better. This further encourages challenging pixels of a class to cluster together and produces sharper decision boundaries, leading to accurate and coherent mask generation in complex scenes. For this, we introduce DQTD, which operates utilizing textual queries consisting of two complementary sets: class-level textual queries, denoted as $Q_{\text{aligned}} \in \mathbb{R}^{(K \cdot L) \times D}$ obtained from PTRM, where $K \cdot L$ signifies the total number of classes multiplied by their abstraction levels, and learnable instance-level queries, represented as $Q_{\text{vis}} \in \mathbb{R}^{M \times D}$, with M indicating the number of object queries and D being the shared embedding width.

Dataset	labelled Data Ratio																ZegCLIP+UniMatch [†]		UniMatch [†]		ZegCLIP [†]		UniMatch-V2		UniMatch-V2			
		PseudoSeg	CPS	ST++	U ² PL	PCR	DualTeacher	ESL	LogicDiag	UniMatch	3-CPS	CuM	AEI	PSeg	PC ²	UniM.	LogicD.	ViT-B / 16	SemVL	Ours	DINOv2-S	DINOv2-B	EVA02-L	Gain				
Backbone		ResNet-101										Xception-60					ViT-B / 16		DINOv2-S		DINOv2-B		EVA02-L					
PASCAL VOC	1/115 (92)	57.6	64.1	65.2	68.0	70.1	70.8	71.0	73.3	75.2	75.7	-	-	-	-	-	-	78.0	77.9	69.3	84.0	87.1	79.0	86.3	89.4	+3.1		
	1/58 (183)	65.5	67.4	71.0	69.2	74.7	74.5	74.0	76.7	77.2	77.7	-	-	-	-	-	-	80.3	80.1	74.2	85.6	88.2	85.5	87.9	90.1	+2.2		
	1/29 (366)	69.1	71.7	74.6	73.7	77.2	76.4	78.1	77.9	78.9	80.1	-	-	-	-	-	-	80.9	82.0	78.7	86.0	88.6	85.9	88.9	90.9	+2.0		
	1/14 (732)	72.4	75.9	77.3	76.2	78.5	77.7	79.5	79.4	79.9	80.9	-	-	-	-	-	-	82.8	83.3	81.0	86.7	89.2	86.7	90.0	91.5	+1.5		
	1/7 (1464)	-	-	79.1	79.5	80.7	78.2	81.8	-	81.2	82.0	-	-	-	-	-	-	83.6	84.0	82.0	87.3	89.9	87.8	90.8	91.8	+1.0		
COCO	1/512 (232)	-	-	-	-	-	-	-	-	-	-	-	-	29.8	29.9	31.9	33.1	-	36.6	-	50.1	54.5	39.3	47.9	59.4	+9.3		
	1/256 (463)	-	-	-	-	-	-	-	-	-	-	-	-	37.1	37.5	38.9	40.3	-	44.1	-	52.8	56.7	45.4	55.8	61.3	+5.5		
	1/128 (925)	-	-	-	-	-	-	-	-	-	-	-	-	39.1	40.1	44.4	45.4	-	49.1	-	53.6	57.5	53.2	58.7	63.7	+5.0		
	1/64 (1.8k)	-	-	-	-	-	-	-	-	-	-	-	-	41.8	43.7	48.2	48.8	-	53.5	-	55.4	59.1	55.0	60.4	65.1	+4.7		
	1/32 (3.7k)	-	-	-	-	-	-	-	-	-	-	-	-	43.6	46.1	49.8	50.5	-	55.0	-	56.5	59.9	57.0	63.3	67.4	+4.1		
ADE20K	1/128 (158)	-	-	-	-	-	-	-	-	-	-	-	-	-	-	15.6	-	18.4	-	-	-	28.1	34.0	-	41.6	+13.5		
	1/64 (316)	-	-	-	-	-	-	-	-	-	-	-	-	-	-	21.6	-	25.3	-	-	-	33.7	38.8	31.5	38.7	43.5	+4.8	
	1/32 (632)	-	-	-	-	-	-	-	-	-	-	-	-	-	-	26.2	28.4	31.2	-	-	-	35.1	39.8	38.1	45.0	48.2	+3.2	
	1/16 (1.3k)	-	-	-	-	-	-	-	-	-	-	-	-	29.8	33.2	-	-	34.4	-	-	-	37.2	41.6	40.7	46.7	49.8	+3.1	
	1/8 (2.5k)	-	-	-	-	-	-	-	-	-	-	-	-	35.6	38.0	-	-	34.6	-	-	-	38.0	39.4	43.3	44.4	49.8	52.6	+2.8
CITYSCAPES	1/30 (100)	61.0	-	-	-	-	-	-	-	-	-	-	-	-	-	-	-	73.8	-	-	-	76.2	78.0	-	79.6	+3.4		
	1/16 (186)	-	69.8	-	74.9	73.4	-	75.1	76.8	76.6	75.7	-	75.8	-	-	-	-	76.6	-	77.9	79.0	80.6	83.6	84.1	84.9	+0.5		
	1/8 (372)	69.8	74.3	-	76.5	76.3	-	77.2	78.9	77.9	77.4	-	77.9	-	-	-	-	78.2	-	79.2	80.4	81.9	84.3	84.9	85.0	+0.6		
	1/4 (744)	72.4	74.6	-	78.5	78.4	-	78.9	80.2	79.2	78.5	-	79.0	-	-	-	-	79.1	-	80.3	81.1	82.4	84.5	85.1	85.0	+0.6		
	1/2 (1.4k)	-	76.8	-	79.1	79.1	-	80.5	81.0	79.5	-	-	80.3	-	-	-	-	79.6	-	80.6	81.3	82.6	85.1	85.3	85.0	+0.2		

Table 1: Comparison of HVL with state-of-the-art semi-supervised segmentation methods on PASCAL VOC, COCO, ADE20K and Cityscapes. The mIoU (%) is reported across varying labelled splits. Best results on Vision-Language based methods are highlighted in red, second-best in blue.

The final step involves updating both class-level and instance-level textual queries and predicting segmentation masks. The transformer decoder, composed of N masked attention layers, refines the initial refined textual queries $Q^{(0)} = Q_{\text{aligned}} \cup Q_{\text{vis}} \in \mathbb{R}^{(K \cdot L + M) \times D}$ into $Q^{(N)} \in \mathbb{R}^{(K \cdot L + M) \times D}$ by integrating pixel features from the pixel decoder. Each refined textual query $q_i \in \mathbb{R}^D$ (where q_i is the i -th query from final set of queries $Q^{(N)}$) predicts a binary mask $\hat{Y}_i \in [0, 1]^{H \times W}$ over the image by computing a dot product with the final per-pixel embedding $F_{\text{pixel}} \in \mathbb{R}^{H \times W \times D}$ from the pixel decoder, followed by sigmoid activation. This results in a set of masks $\hat{Y} \in \mathbb{R}^{H \times W \times (K \cdot L + M)}$, where each query focuses on different parts of the image based on the semantic or visual patterns it has learned.

In parallel, each query from $Q^{(N)}$ is assigned a class label using a linear classifier applied to the query embedding. To construct the final segmentation map, we select, for each pixel, the query with the highest mask response at that location and assign its predicted class label to the pixel. This produces a coherent semantic segmentation map $\hat{Y}_{\text{final}} \in \mathbb{R}^{H \times W}$, where each pixel is assigned a single class index.

Following Cheng et al. [2022], we train the HVL framework using a segmentation loss \mathcal{L}_{seg} :

$$\mathcal{L}_{\text{seg}} = \lambda_{\text{ce}} \mathcal{L}_{\text{ce}} + \lambda_{\text{dice}} \mathcal{L}_{\text{dice}} + \lambda_{\text{class}} \mathcal{L}_{\text{class}}, \quad (1)$$

where \mathcal{L}_{ce} and $\mathcal{L}_{\text{dice}}$ supervise the predicted masks and $\mathcal{L}_{\text{class}}$ optimizes the class prediction for each query. For unlabelled images, we apply the entropy minimization defined in Nadeem et al. [2025a]. Moreover, we adopt a fixed matching strategy for query assignment, where each class-level textual query is permanently assigned to a specific semantic class throughout training, thus each class-level query represents the semantic information of only one class, while allowing instance-level queries to capture visual diversity within and across classes. To preserve semantic meaning of learned prompt query regularization including topology loss and anchor loss are applied. **Regularization Objectives.**

We introduce two complementary regularization objectives, each applied independently to respective encoders, designed to maintain alignment between the visual and textual features. It includes (1) *query regularization* that preserves the semantic meaning of learned prompts relative to their original text embeddings. (2) *segmentation supervision* that trains the model to produce accurate and coherent binary masks using pixel-wise losses, and (3) *classification supervision* that ensures each query predicts a consistent class label aligned with the textual embedding space.

Query Regularization. Learning prompts improve segmentation but may distort the original CLIP’s text embeddings with domain-invariant semantics. To preserve this semantic alignment, we introduce a regularization loss targeted at the prompt generator, that ensures consistency between learned prompt embeddings and fixed text embeddings. We define this as an elastic alignment problem where $\mathcal{L}_{\text{topo}}$ maintains relative angles between class embeddings and $\mathcal{L}_{\text{anchor}}$ keeps each learned prompt close to its CLIP prototype while separating it from others given as: $\mathcal{L}_{\text{topo}} = \sum_{i=1}^K \sum_{j=1}^K (\hat{t}_i^\top \hat{t}_j - \hat{t}_i^{\text{CLIP}^\top} \hat{t}_j^{\text{CLIP}})^2$, $\mathcal{L}_{\text{anchor}} = \sum_{k=1}^K [\|\Phi(\hat{t}_k) - \hat{t}_k^{\text{CLIP}}\|_2 - \sum_{j \neq k} \log(1 + \|\Phi(\hat{t}_k) - \Phi(\hat{t}_j)\|_2)]$, $\mathcal{L}_{\text{prompt}} = \mathcal{L}_{\text{topo}} + \mathcal{L}_{\text{anchor}}$.

Here, \hat{t}_k and \hat{t}_k^{CLIP} are the normalized embeddings from frozen E_T i.e. CLIP, from the learnable and fixed prompts for class k , and Φ is a learnable prompt generator i.e. two-layer MLP. This loss prevents prompts from distorting the semantic space of original CLIP text embeddings while allowing them to adapt to the segmentation task.

Segmentation Supervision. [reduce length] To improve the segmentation capability of textual queries, we aim to strengthen pixel-level vision-language alignment. This alignment can deteriorate when the visual encoder E_I overfits to local patterns, especially under domain shifts. To mitigate this, we adopt a masked consistency strategy that enhances the E_I ability to rely on language when visual evidence is incomplete.

Specifically, we randomly mask all pixels of a target class in the input image and pass the masked image through the learnable encoder E_I^θ to obtain masked features x_{mask} . The unmasked image is simultaneously processed by a frozen encoder E_I^0 to yield reference features x_{ref} . Masked image consistency loss minimizes cosine distance on the masked region $M \subset \{1, \dots, H \times W\}$: $\mathcal{L}_{\text{mask}} = \frac{1}{|M|} \sum_{i \in M} (1 - \cos(x_{\text{mask},i}, x_{\text{ref},i}))$. To ensure that the model still relies on the language signal under occlusion, we apply a pixel-level contrastive loss over the masked region, aligning features with their class text embeddings: $\mathcal{L}_{\text{align}} = -\frac{1}{|M|} \sum_{i \in M} \log \frac{e^{\cos(x_{\text{mask},i}, t_{k_i})/\tau}}{\sum_{k=1}^K e^{\cos(x_{\text{mask},i}, t_k)/\tau}}$, where t_{k_i} is the CLIP text embedding for the true class at pixel i , and τ is a temperature scaling parameter. The final loss for masked vision-language regularization is: $\mathcal{L}_{\text{vl}} = \mathcal{L}_{\text{align}} + \lambda_{\text{mask}} \mathcal{L}_{\text{mask}}$. The weight λ_{mask} is chosen from Nadeem et al. [2025a]. This strategy aligns the model with language, even when visual information is occluded, thus improving robustness and generalization for open-vocabulary segmentation.

4 Experiments

4.1 Implementation Details

Network Architecture. Our model leverages encoder E_I (patch size = 16) Dosovitskiy et al. [2020] and a Transformer text encoder E_T Vaswani et al. [2017], both initialized with either CLIP Radford et al. [2021a] or EVA02-CLIPSun et al. [2023]. The CLIP utilizes Vision Transformer-base (ViT-B) backbone with a patch size of 16, while EVA02-CLIP utilizes EVA02-large backbone with a patch size of 14. The multi-scale pixel decoder is adopted from DN-DETR Li et al. [2022], with PTRM interleaved after each Deformable-Attention(D.Attn) layer with M=6 layers. An 8-token learnable prompt p is prepended to each encoder sequence to specialize the joint representation for segmentation. For the Dual-Query Transformer Decoder, we follow the Mask2Former’s Cheng et al. [2022] default settings, consisting of N=9 layers along with masked attention. Our framework inherits CLIP’s biases and may struggle with domain-specific classes absent in training data, limiting domains adaptation.

Training. We benchmark **HVL** on Pascal VOC Everingham et al. [2010], COCO Lin et al. [2014], ADE20K Zhou et al. [2017], and Cityscapes Cordts et al. [2016] using a two 24 GB NVIDIA GeForce RTX-3090. Following the semi-supervised setting of SemiVL, each iteration processes a mixed batch of eight labelled and eight unlabelled images. Inputs are randomly cropped to 512×512 pixels, except for Cityscapes, where we adopt the crop of 801×801 . Optimization employs AdamW for 80, 10, 40, 240 epochs on VOC, COCO, ADE20K, Cityscapes, respectively, with a 0.9 polynomial learning-rate decay and base learning rate of 10^{-4} . We set the learning rate to 1×10^{-4} with the backbone learning rate reduced by a factor of 0.1. Linear warm-up Nadeem et al. [2025b] is applied over $t_{\text{warm}} = 1.5\text{k}$ iterations, followed by a linear decay. We apply standard augmentations for segmentation tasks, including random scaling, random cropping, random flipping, and color jittering. Additionally, we adopt rare class sampling, following Nadeem et al. [2025a]. Moreover, we instantiate one textual query per class (e.g., 19 for Cityscapes), each prefixed by an eight-token learnable prompt

4.2 Comparison with the SOTA Methods

Pascal VOC. On Pascal VOC (10582 train images; 1464 labelled), we vary the labelled images from 92 to 1464 images. As shown in Tab. 1, HVL improves mIoU by 3.1% at 92 labels and 2.6% at 1464 labels over SemiVL and 2.2% over UniMatch-v2, demonstrating that utilizing textual queries as an anchor for grouping pixels of similar class deliver substantial benefits in low-annotation

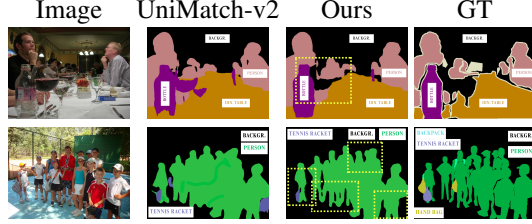


Figure 5: The Pascal VOC with 92 labels (top) and COCO with 232 labels (bottom). HVL correctly disambiguates visually similar classes, suppresses over-segmentation in cluttered regions, produces sharp object boundaries, and accurately identify multiple persons in dense crowds.

Model	Scores																							
UniMatch(Vit)	93	94	69	94	78	76	91	88	94	19	96	56	90	93	82	88	61	94	21	88	71			
SemiVL	89	96	78	95	84	84	95	85	97	37	97	72	93	95	90	92	73	94	59	91	68			
Ours(Without HTQG)	91	96	79	97	86	88	95	87	97	43	97	78	94	95	92	93	77	95	64	90	71			
Ours	94	97	79	97	88	90	95	91	97	48	97	78	94	95	92	93	81	95	67	91	73			
	Airplane Backgr. Bicycle Bird Boat Bottle Bus Car Cat Chair Cow Din. Table Dog Horse M.bike Person Plant Sheep Sofa Train Monitor																							

Table 2: Class-Wise IoU Scores

regimes. A class-wise breakdown in Tab 1 reveals that the most significant gains occur on visually ambiguous categories, such as chair, dining table, and sofa, where SemiVL and UniMatch[†] frequently make errors. These results are also evident in Fig.5, where our HVL correctly distinguishes a sofa and a chair, while previous SOTA struggles. An ablation without HTQG shows that incorporating hierarchical query yields additional IoU boosts of roughly 3–7% on the most challenging classes, proving that intra-class variability can be tackled by adding coarse-to-fine textual queries.

COCO. On COCO (118k train images; 81 classes), the diversity of categories substantially raises the difficulty of semi-supervised learning. Here, HVL’s language–vision integration excels at disentangling a wide range of semantic concepts, yielding a +9.3% mIoU gain with only 232 labels.

ADE20K. ADE20K (20.21k train images; 150 classes) presents an even broader scene-parsing challenge. Table 1 shows that HVL achieves up to +13.5% mIoU with only 158 labels, further validating its effectiveness.

Cityscapes. Finally, on Cityscapes (2.975k train images; 19 classes), HVL outperforms SemiVLHoyer et al. [2024] by up to +1.8% and UniMatch-v2 by +3.4% mIoU at 100 labels as shown in Table 1. These gains, though smaller, are noteworthy given the prevalence of fine-grained street-scene classes (e.g., distant poles, traffic signs) that are especially challenging under sparse caption guidance.

4.3 Analysis

Ablation. Tab. 3 quantifies the contributions of the components, beginning with the Mask2Former baseline of 82.0/83.3 mIoU₉₂/mIoU₁₄₆₄ with randomly initialized object queries. We evaluated the effect of generating domain-invariant semantic cue based object queries (textual queries) and eliminating absent class queries; the results show the largest performance gain of +2.9/ + 4.8%. This proves that directly utilizing randomly initialized random object queries results in sub-optimal performance, while adding semantic priors from VLMs yields enhanced textual query generation and thus effective segmentation. Then, we examine the contribution of refining pixel features in a pixel decoder through textual queries - unlike prior methods like Mask2Former-PTRM (Q_{aligned}). It elevates the performance by +0.7/ + 0.6 %. Moreover, the study reveals an increase of +0.9/ + 0.6 % depicting the supremacy of including object queries at the instance level, i.e., $Q_{\text{aligned}} \cup Q_{\text{vis}}$, depicting that it enhances the intra-class variability. Furthermore, the inclusion of combined query refinement results in further +0.6/ + 0.6%. Stronger gains for 92 labels (+5.1 % vs. +5.6 % for 1464) stem from domain-invariant textual query generation and pixel feature semantic clarity enhancement through them, thus, compensating for sparse supervision.

Regularization. Tab. 4 evaluates our regularization losses on Pascal VOC. The masked consistency loss $\mathcal{L}_{\text{mask}}$ proves the most critical for the robustness of the occlusion. In contrast, the prompt topology

Random Object Queries	HTQG Q_{text}	PTRM Q_{aligned}	$Q^{(0)}$	DQTD $Q^{(N_{\text{dec}})}$	mIoU ₉₂	mIoU ₁₄₆₄
✓	—	—	—	—	82.0	83.3
—	✓	—	—	—	84.9	88.1
—	✓	✓	—	—	85.6	88.7
—	✓	✓	✓	—	86.5	89.3
—	✓	✓	✓	✓	87.1	89.9

Table 3: Ablation on VOC (mIoU₉₂/mIoU₁₄₆₄). Our domain-invariant textual queries enhance the performance over a randomly initialized query-based baseline.

Row	$\mathcal{L}_{\text{prompt}}$	$\mathcal{L}_{\text{mask}}$	$\mathcal{L}_{\text{align}}$	mIoU ₉₂
1	—	✓	✓	86.0
2	✓	—	✓	85.2
3	✓	✓	—	84.7
4	✓	✓	✓	87.1

Table 4: Regularization Ablation (mIoU₉₂). All the losses contribute to the improvement of results.

loss $\mathcal{L}_{\text{prompt}}$ maintains the semantic relationships of CLIP, and the alignment loss $\mathcal{L}_{\text{align}}$ strengthens the local pixel-text correspondence. They show complementary benefits: prompt loss preserves global semantics, masked loss ensures feature stability, and alignment loss refines localization, collectively boosting performance by 2.4 mIoU.

5 Conclusion

HVL presents a novel and unified framework for SSS. By integrating domain-invariant semantics from vision–language models as hierarchical textual queries and refining them through HTQG, PTRM, and DQTD, HVL achieves precise robust class discrimination with minimal supervision.

References

- Rabab Abdelfattah, Qing Guo, Xiaoguang Li, Xiaofeng Wang, and Song Wang. Cdul: Clip-driven unsupervised learning for multi-label image classification. In *Proceedings of the IEEE/CVF international conference on computer vision*, pages 1348–1357, 2023.
- Liang-Chieh Chen, Yukun Zhu, George Papandreou, Florian Schroff, and Hartwig Adam. Encoder-decoder with atrous separable convolution for semantic image segmentation. In *Proceedings of the IEEE/CVF Conference on Computer Vision and Pattern Recognition (CVPR)*, 2023a.
- Xiaokang Chen, Yuhui Yuan, Gang Zeng, and Jingdong Wang. Semi-supervised semantic segmentation with cross pseudo supervision. In *Proceedings of the IEEE/CVF Conference on Computer Vision and Pattern Recognition (CVPR)*, pages 2613–2622, 2021.
- Zhe Chen, Jiannan Wu, Chen Wang, et al. Internvl: Scaling up vision foundation models and aligning for generic visual-linguistic tasks. *arXiv preprint arXiv:2312.14238*, 2023b.
- Bowen Cheng, Ishan Misra, Alexander G Schwing, Alexander Kirillov, and Rohit Girdhar. Masked-attention mask transformer for universal image segmentation. In *CVPR*, pages 1290–1299, 2022.
- H. Chi, J. Pang, B. Zhang, and W. Liu. Adaptive bidirectional displacement for semi-supervised medical image segmentation. In *Proceedings of the IEEE/CVF Conference on Computer Vision and Pattern Recognition (CVPR)*, pages 4070–4080, 2024. doi: 10.1109/CVPR52717.2024.00395.
- Marius Cordts, Mohamed Omran, Sebastian Ramos, Timo Rehfeld, Markus Enzweiler, Rodrigo Benenson, Uwe Franke, Stefan Roth, and Bernt Schiele. The cityscapes dataset for semantic urban scene understanding. In *CVPR*, pages 3213–3223, 2016.
- Alexey Dosovitskiy, Lucas Beyer, Alexander Kolesnikov, Dirk Weissenborn, Xiaohua Zhai, Thomas Unterthiner, Mostafa Dehghani, Matthias Minderer, Georg Heigold, Sylvain Gelly, et al. An image is worth 16x16 words: Transformers for image recognition at scale. *arXiv preprint arXiv:2010.11929*, 2020.
- Mark Everingham, Luc Van Gool, Christopher KI Williams, John Winn, and Andrew Zisserman. The pascal visual object classes (voc) challenge. *IJCV*, 88(2):303–338, 2010.
- Yuxin Fang, Wen Wang, Binhui Xie, Quan Sun, Ledell Wu, Xinggang Wang, Tiejun Huang, Xinlong Wang, and Yue Cao. Eva-clip: Improved training techniques for clip at scale. *arXiv*, 2023.

- G. French, T. Aila, S. Laine, M. Mackiewicz, and G. Finlayson. Semi-supervised semantic segmentation needs strong, high-dimensional perturbations. In *Proceedings of the British Machine Vision Conference (BMVC)*, 2020. URL <https://www.bmvc2020-conference.com/programme/>. Virtual Conference.
- Geoffrey French, Samuli Laine, Timo Aila, Tero Karras, and Jaakko Lehtinen. Improving few-shot learning by training on image differences. In *Proceedings of the IEEE/CVF International Conference on Computer Vision (ICCV)*, 2019.
- D. Guan, J. Huang, A. Xiao, and S. Lu. Unbiased subclass regularization for semi-supervised semantic segmentation. In *Proceedings of the IEEE/CVF Conference on Computer Vision and Pattern Recognition (CVPR)*, pages 9958–9968, 2022. doi: 10.1109/CVPR52688.2022.00973.
- Lukas Hoyer, Dengxin Dai, and Luc Van Gool. Semivl: Semi-supervised semantic segmentation with vision-language guidance. pages 1234–1243, 2024.
- H. Hu, F. Wei, H. Hu, Q. Ye, J. Cui, and L. Wang. Semi-supervised semantic segmentation via adaptive equalization learning. In *Advances in Neural Information Processing Systems (NeurIPS)*, pages 22106–22118, 2021. URL <https://proceedings.neurips.cc/paper/2021/hash/> . . .
- Menglin Jia, Luming Tang, Bor-Chun Chen, Claire Cardie, Serge Belongie, Bharath Hariharan, and Ser-Nam Lim. Visual prompt tuning. In *ECCV*, pages 709–727, 2022. doi: 10.1007/978-3-031-19809-0_41.
- A. Kamath, M. Singh, Y. LeCun, G. Synnaeve, I. Misra, and N. Carion. Mdettr – modulated detection for end-to-end multi-modal understanding. In *IEEE/CVF International Conference on Computer Vision (ICCV)*, pages 1780–1790, 2021. doi: 10.1109/ICCV48922.2021.00183.
- Feng Li, Hao Zhang, Shilong Liu, Jian Guo, Lionel M Ni, and Lei Zhang. Dn-detr: Accelerate detr training by introducing query denoising. In *CVPR*, pages 13619–13627, 2022.
- Tsung-Yi Lin, Michael Maire, Serge Belongie, James Hays, Pietro Perona, Deva Ramanan, Piotr Dollár, and C Lawrence Zitnick. Microsoft coco: Common objects in context. *ECCV*, pages 740–755, 2014.
- Haotian Liu, Chunyuan Li, Qingyang Wu, and Yong Jae Lee. Visual instruction tuning. *arXiv preprint arXiv:2304.08485*, 2023.
- Yuchao Liu, Yuhua Tian, Yaowei Chen, Fengguang Liu, Vasileios Belagiannis, and Gustavo Carneiro. St++: Make self-training work better for semi-supervised semantic segmentation. In *Proceedings of the IEEE/CVF Conference on Computer Vision and Pattern Recognition (CVPR)*, pages 4268–4277, 2022.
- Sudhanshu Mittal, Maxim Tatarchenko, and Thomas Brox. Semi-supervised semantic segmentation with high- and low-level consistency. *IEEE transactions on pattern analysis and machine intelligence*, 43(4):1362–1379, 2019.
- Numair Nadeem, Muhammad Hamza Asad, Saeed Anwar, and Abdul Bais. Maskadapt: Unsupervised geometry-aware domain adaptation using multimodal contextual learning and rgb-depth masking. In *Proceedings of the Computer Vision and Pattern Recognition Conference (CVPR) Workshops*, pages 5422–5432, June 2025a.
- Numair Nadeem, Muhammad Hamza Asad, and Abdul Bais. Robust uda for crop and weed segmentation: Multi-scale attention and style-adaptive techniques. In Alessio Del Bue, Cristian Canton, Jordi Pont-Tuset, and Tatiana Tommasi, editors, *Computer Vision – ECCV 2024 Workshops*, pages 284–302, Cham, 2025b. Springer Nature Switzerland.
- Byeonghyun Pak, Byeongju Woo, Sunghwan Kim, Dae-hwan Kim, and Hoseong Kim. Textual query-driven mask transformer for domain generalized segmentation. In *Proceedings of the European Conference on Computer Vision (ECCV)*, pages 1234–1245. Springer, 2024. URL <https://example.com/paper-url>. Equal contribution and Corresponding author markers.
- Alec Radford, Jong Wook Kim, Chris Hallacy, Aditya Ramesh, Gabriel Goh, Sandhini Agarwal, Girish Sastry, Amanda Askell, Pamela Mishkin, Jack Clark, et al. Learning transferable visual models from natural language supervision. *arXiv preprint arXiv:2103.00020*, 2021a.
- Alec Radford, Jong Wook Kim, Chris Hallacy, Aditya Ramesh, Gabriel Goh, Sandhini Agarwal, Girish Sastry, Amanda Askell, Pamela Mishkin, Jack Clark, et al. Learning transferable visual models from natural language supervision. In *Proceedings of the 38th International Conference on Machine Learning (ICML)*, volume 139, pages 8748–8763. PMLR, 2021b. URL <https://proceedings.mlr.press/v139/radford21a.html>.
- Kihyuk Sohn, David Berthelot, Nicholas Carlini, Zizhao Zhang, Han Zhang, Colin A Raffel, Ekin Dogus Cubuk, Alexey Kurakin, and Chun-Liang Li. Fixmatch: Simplifying semi-supervised learning with consistency and confidence. *Advances in Neural Information Processing Systems (NeurIPS)*, 33:596–608, 2020.
- Nasim Souly, Concetto Spampinato, and Mubarak Shah. Semi supervised semantic segmentation using generative adversarial network. In *Proceedings of the IEEE International Conference on Computer Vision (ICCV)*, pages 5688–5696, 2017.
- Yuxin Sun, Li Dong, Shaohan Huang, Shuming Ma, Yuqing Xia, Anxiang Xue, Jiahui Wang, and Furu Wei. Eva-02: A visual representation for neon genesis. *arXiv preprint arXiv:2303.11331*, 2023.

- Jiaming Tao, Yutao Wang, Xinyu Li, Xiaobo Wang, and Xinggang Wang. Cat-seg: Cost aggregation for open-vocabulary semantic segmentation. In *ICCV*, pages 11783–11793, 2023. doi: 10.1109/ICCV51070.2023.01086.
- Ashish Vaswani, Noam Shazeer, Niki Parmar, Jakob Uszkoreit, Llion Jones, Aidan N Gomez, Łukasz Kaiser, and Illia Polosukhin. Attention is all you need. *NeurIPS*, 30, 2017.
- L. Wu, L. Fang, X. He, M. He, J. Ma, and Z. Zhong. Querying labeled for unlabeled: Cross-image semantic consistency guided semi-supervised semantic segmentation. *IEEE Transactions on Pattern Analysis and Machine Intelligence*, 45(7):8827–8844, Jul. 2023. doi: 10.1109/TPAMI.2022.3223738.
- Jiarui Xu, Shalini De Mello, Sifei Liu, Wonmin Byeon, Thomas Breuel, Jan Kautz, and Xiaolong Wang. Groupvit: Semantic segmentation emerges from text supervision. In *CVPR*, pages 18134–18144, 2022. doi: 10.1109/CVPR52688.2022.01762.
- L. Yang, Z. Zhao, L. Qi, Y. Qiao, Y. Shi, and H. Zhao. Shrinking class space for enhanced certainty in semi-supervised learning. In *Proceedings of the IEEE/CVF International Conference on Computer Vision (ICCV)*, pages 16141–16150, 2023a. doi: 10.1109/ICCV51070.2023.01485.
- Lei Yang, Lei Qi, Litong Feng, Wayne Zhang, and Yuxin Shi. Revisiting weak-to-strong consistency in semi-supervised semantic segmentation. In *Proceedings of the IEEE/CVF Conference on Computer Vision and Pattern Recognition (CVPR)*, pages 7236–7246, 2023b. doi: 10.1109/CVPR52729.2023.00700.
- Lihe Yang, Wei Zhuo, Lei Qi, Yinghuan Shi, and Yang Gao. St++: Make self-training work better for semi-supervised semantic segmentation. In *Proceedings of the IEEE/CVF Conference on Computer Vision and Pattern Recognition (CVPR)*, pages 4268–4277, 2022.
- Lihe Yang, Zhen Zhao, and Hengshuang Zhao. Unimatch v2: Pushing the limit of semi-supervised semantic segmentation. *IEEE Transactions on Pattern Analysis and Machine Intelligence*, 47(4):3031–3048, 2025a. doi: 10.1109/TPAMI.2025.3528453.
- Lihe Yang, Zhen Zhao, and Hengshuang Zhao. Unimatch v2: Pushing the limit of semi-supervised semantic segmentation. *IEEE Transactions on Pattern Analysis and Machine Intelligence*, 2025b.
- Q. Yu, H. Wang, S. Qiao, M. Collins, Y. Zhu, H. Adam, A. Yuille, and L. C. Chen. kmax-deeplab: k-means mask transformer. In *European Conference on Computer Vision (ECCV)*, pages 282–299, 2022. doi: 10.1007/978-3-031-19809-0_17.
- J. Yuan, Y. Liu, C. Shen, Z. Wang, and H. Li. A simple baseline for semi-supervised semantic segmentation with strong data augmentation. In *Proceedings of the IEEE/CVF International Conference on Computer Vision (ICCV)*, pages 8209–8218, 2021. doi: 10.1109/ICCV48922.2021.00812.
- S. Yuan, R. Zhong, C. Yang, Q. Li, and Y. Dong. Dynamically updated semi-supervised change detection network combining cross-supervision and screening algorithms. *IEEE Transactions on Geoscience and Remote Sensing*, 62:1–14, 2024. doi: 10.1109/TGRS.2024.3360894.
- S. Yun, D. Han, S. J. Oh, S. Chun, J. Choe, and Y. Yoo. Cutmix: Regularization strategy to train strong classifiers with localizable features. In *Proceedings of the IEEE/CVF International Conference on Computer Vision (ICCV)*, pages 6022–6031, 2019. doi: 10.1109/ICCV.2019.00612.
- H. Zhang, F. Li, H. Xu, S. Huang, S. Liu, L. M. Ni, and L. Zhang. Mp-former: Mask-piloted transformer for image segmentation. In *IEEE/CVF Conference on Computer Vision and Pattern Recognition (CVPR)*, pages 18384–18394, 2023a. doi: 10.1109/CVPR52717.2023.01762.
- Wenwei Zhang, Tai Zhou, Lu Qi, Donglian Jiang, Jifeng Lu, and Jiaya Jia. Zegclip: Towards adapting clip for zero-shot semantic segmentation. In *CVPR*, pages 11175–11185, 2023b. doi: 10.1109/CVPR52717.2023.01075.
- Z. Zhao, S. Long, J. Pi, J. Wang, and L. Zhou. Instance-specific and model-adaptive supervision for semi-supervised semantic segmentation. In *Proceedings of the IEEE/CVF Conference on Computer Vision and Pattern Recognition (CVPR)*, pages 23705–23714, 2023. doi: 10.1109/CVPR52717.2023.02271.
- Z. Zhao, Z. Wang, L. Wang, Y. Yuan, and L. Zhou. Alternate diverse teaching for semi-supervised medical image segmentation. In *Proceedings of the European Conference on Computer Vision (ECCV)*, pages 227–243, 2024. doi: 10.1007/978-3-031-50078-7_14.
- Ziwen Zhong, Yuxuan Lin, Jianfeng Wu, and Hong Wang. Understanding imbalanced semantic segmentation through neural collapse. In *Proceedings of the IEEE/CVF Conference on Computer Vision and Pattern Recognition (CVPR)*, 2023.
- Bolei Zhou, Hang Zhao, Xavier Puig, Sanja Fidler, Adela Barriuso, and Antonio Torralba. Scene parsing through ade20k dataset. *CVPR*, pages 633–641, 2017.
- Chong Zhou, Chen Change Loy, and Bo Dai. Extract free dense labels from clip. In *Proceedings of the European Conference on Computer Vision (ECCV)*, 2022a.

- Kaiyang Zhou, Jingkang Yang, Chen Change Loy, and Ziwei Liu. Conditional prompt learning for vision-language models. In *CVPR*, pages 16816–16825, 2022b. doi: 10.1109/CVPR52688.2022.01633.
- Kaiyang Zhou, Jingkang Yang, Chen Change Loy, and Ziwei Liu. Coop: Learning to prompt for vision-language models. *International Journal of Computer Vision*, 130:2337–2348, 2022c. doi: 10.1007/s11263-022-01653-1.
- Y. Zou et al. Pseudoseg: Designing pseudo labels for semantic segmentation. In *Proceedings of the International Conference on Learning Representations (ICLR)*, 2021. URL <https://openreview.net/forum?id=K81UvFqS2A>. Conference Track.